Gamma-ray attenuation properties carbide compounds (WC, Mo2C, TiC, SiC, B4C) using Phy-X/PSD software

Iskender Akkurt[1], Kadir Günoğlu[2*]

[1]Süleyman Demirel Üniversity, Science and Arts Faculty, Physics Department, 32200, Isparta-Turkiye
Email: iskenderakkurt@sdu.edu.tr - **ORCID:** 0000-0002-5247-7850

[2] Isparta University of Applied Sciences, Technical Vocational School, 32200, Isparta-Turkiye
* **Corresponding Author Email:** kadirgnoglu@gmail.com **- ORCID:** 0000-0002-9008-9162

Abstract: As a result of the increase in the use of radiation in many application areas, it has become an important need to carry out effective studies on protection from the harmful effects of radiation. The vast majority of studies on radiation protection are based on the principle of reducing and/or holding different types of radiation using a shielding material. The main purpose of this study is to evaluate the gamma ray shielding properties of different carbide compounds (such as WC, Mo2C, TiC, SiC, B4C) by using Phy-X/PSD software at gamma ray energies between 0.015 and 15 MeV. To determine the shielding properties of carbide samples in the mentioned energy range, parameters such as linear (LAC) and mass (MAC) attenuation coefficients, mean free path (MFP), half value (HVL) and tenth value (TVL) were calculated.

1. Introduction

Among the terms used most frequently in both organic and inorganic chemistry is "carbide." Let's tackle the main question now: what is carbide? Carbide is a chemical compound composed of metal or semi-metallic elements and carbon. It exists as an ionic form. The carbide group is attached to the metal or semi-metal element by an ionic or covalent bond. The carbides can be divided into several groups according to the type of bond that forms between the carbide ion and the metal or semi-metallic element [1].

- **Ionic carbides:** Highly electropositive elements such as alkali metals or alkaline earth metals combine with carbide ions to form ionic carbides. The strong electrostatic force attracts these ions to one another. There is a significant electronegativity difference in this kind of ionic carbide. Calcium carbide is one type of ionic carbide [1].

- **Covalent carbides:** Low electropositive elements like silicon and boron combine to form covalent carbides. There are little variations in their electronegativity. Silicon carbide and boron carbide are two instances of covalent carbides [1].

- **Interstitial carbides:** They are formed with certain lanthanides and transition metals such as Cr, Mn, Fe, Co, Ti, and W. In general, they melt quickly and are hard. The C atoms do not change the metal's conductivity because they are positioned in octahedral voids within the metal lattice. Carbon atoms' undistorted entry into the metal lattice suggests that the interstices should be fairly large (possible if the metal's atomic radius is greater than 135 pm). When carbon is added to smaller metals, such as those in the 3d series, the lattice is distorted and complex structures arise [1].

- **Intermediate transition metal carbides:** The transition metal ion in these carbides is smaller than the critical value of 135 pm, and the structures are more complex rather than interstitial. Several stoichiometries are typical. Iron, for instance, can combine to form the carbides Fe3C, Fe7C3, and Fe2C. The most well-known of these is found in steels and is called cementite (Fe3C). Compared to interstitial carbides, these carbides exhibit greater reactivity. For instance, diluted acids and occasionally water can hydrolyze the carbides of Cr, Mn, Fe, Co, and Ni to produce a mixture of hydrogen and hydrocarbons. These substances have characteristics in common with the more reactive, salt-like carbides as well as the inert interstitials [1].

Human exposure to ionizing radiation has increased as a result of the exponential growth in the use of radioactive sources in a variety of fields, including agriculture, industry, space exploration, medicine, and energy production, as well as technological and communication advancements. Extended exposure could be detrimental to the body's systems. Direct ionizing radiation includes particles like alpha, beta, and proton; indirect ionizing radiation includes neutrons, γ-rays, and X-rays [2-5]. In settings like nuclear power plants, hospitals, and laboratories where ionizing radiation is present, radiation protection shields people's health. Thus, it is essential to use the right protective materials to ensure efficient management of radiation waste in addition to minimizing the harmful biological effects of radiation. By obstructing direct ionizing radiation from outside sources, protection against indirect ionizing radiation is typically adequate. In this regard, low-density structural materials are continuously sought after by materials scientists and engineers in order to reduce energy usage, operational costs, and risks associated with radiation [6,7]. In the field of radiation protection, materials with qualities like high density, melting temperature, mechanical strength, corrosion resistance, and low cost are especially crucial. Due to its high density and atomic number (Z), lead (Pb) is a common element used for radiation protection; however, it has drawbacks, including high toxicity, low melting point, and poor mechanical strength. It is insufficient for radiation protection applications on its own due to these factors [8-11]. Because the effects of radiation vary depending on the type and energy of the radiation, understanding how the material reacts to radiation is crucial for radiation protection. The mass attenuation coefficient (MAC) is one of the most important variables in the interaction between photons and matter. The Beer-Lambert law is used to calculate the attenuation of a monoenergetic photon beam that is passing through a thin layer of the sample. The fundamental ideas of mean free path (MFP), half value (HVL), and tenth value thickness (TVL) are required to comprehend radiation penetration following gamma ray interaction with matter [12].

Ionizing radiation technology is being used more often these days, particularly in industrial and medical settings. Owing to this rise, numerous scientists have been working on creating various shield materials to lessen the negative effects of ionizing radiation. Materials like various composites (compounds and mixtures), alloys, concretes, glasses, and polymers are typically included in these shield materials [13-58].

In the present research, the radiation attenuation parameters of some carbide compounds belonging to different classes were determined theoretically using Phy-X/PSD software [59]. First of all, the linear (LAC) and mass (MAC) attenuation coefficients of carbide compounds were calculated. Thickness parameters such as mean free path (MFP), half value (HVL) and tenth value (TVL) were calculated using the linear attenuation coefficient (LAC).

2. Materials and Methods

The interaction mechanisms of photons with matter differ from the interaction mechanisms of charged particles. As a photon enters a material, some of them are absorbed, some are transmitted through the material without interacting, and others are dispersed away from the original photon, as is the case with low-energy photons. The incident photon energy, shield material, and experimental conditions all have a significant impact on the likelihood that these activities will take place. More attenuation indicates a preferred shielding material for a given thickness. Thus, the Lambert-Beer law's expression of attenuation is the primary factor in determining the choice of shielding material. The Beer-Lambert law, the law of exponential attenuation, is formulated as follows for the variation between the incident and transmitted gamma-ray intensities of a given thickness of material [12].

$$I = I_0 e^{-\mu x} \tag{1}$$

$$LAC(\mu, cm^{-1}) = \frac{1}{x} Ln \frac{I_0}{I} \tag{2}$$

where I_0 is the gamma intensity emitted from the radioactive source, I is the attenuated gamma intensities obtained by placing the shield material between detector and radioactive source, μ (cm^{-1}) is the linear attenuation coefficient (LAC) and x is the thickness of the shield material.

The mass attenuation coefficient (MAC) μ/ρ in cm^2g^{-1} is given as the ratio between the linear attenuation coefficient μ and the density of the shield material. The MAC μ/ρ for any composite material is given by the following relationship at a given photon energy:

$$\mu_m = (\mu/\rho) = \sum_i w_i \, (\mu/\rho)_i \tag{3}$$

where wi and $(\mu/\rho)i$ are the weight fraction (% Wf.) and MAC of the ith element in the chemical composition of the shield material. It is possible to calculate the wi values with the equation given below.

$$w_i = \frac{A_i a_i}{\sum_i A_i a_i} \tag{4}$$

where Ai and ai are the atomic weight and atomic number of the ith element in the composition of the shield material, respectively.

The Phy-X/PSD database can determine shielding values for photon energies between 0.015MeV and 100GeV for any material's molecular or elemental structure [59]. The software accounts for the chemical makeup and density of the constituents while calculating these characteristics. Different shielding parameters such as MAC, LAC, MFP, HVL and TVL can be calculated for each material using theoretical MAC values.

Thickness parameters such as mean free path (MFP, λ), half value layer (HVL, $X_{1/2}$), and tenth value layer (TVL, $X_{1/10}$) are used to determine the radiation shielding characteristics of materials, and these thickness parameters are calculated as an inverse function of the linear attenuation coefficient of the shield material. HVL, TVL and MFP are defined as required material thickness values that reduce the radiation intensity on the material to 10%, 50% and 36.8%, respectively. Equation (5)-(7) is used to calculate these parameters mathematically.

$$MFP \, (\lambda, cm) = \frac{1}{\mu} \tag{5}$$

$$HVL(X_{1/2}, cm) = \frac{Ln2}{\mu} \tag{6}$$

$$TVL(X_{1/10}, cm) = \frac{Ln10}{\mu} \tag{7}$$

3. Results and Discussions

Gamma ray attenuation parameters of the carbide samples selected within the scope of the study were obtained using Phy-X/PSD software. The results obtained for MAC and LAC values are shown in Figure 1.
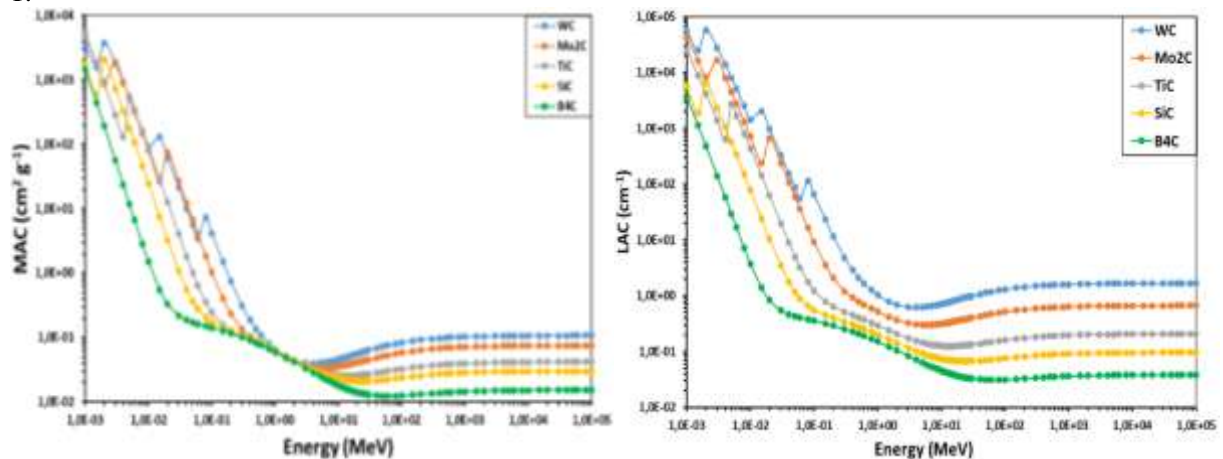

Figure 1. *LAC and MAC values as a function of photon energy for carbide samples.*

As seen in Figure 1, the highest values for both MAC and LAC values were obtained in the WC sample and the lowest values were obtained in the B$_4$C sample. Also in Figure 1, the LAC and MAC values obtained for all samples vary depending on the energy of the interacting gamma rays. This change can be explained as the decrease of LAC and MAC values against increasing gamma ray energy.

Theoretical results obtained in a wide photon energy range appear to result from different interactions in different energy regions. That is, there is a sharp decrease in attenuation at photon energies lower than 0.1 MeV (low energy region), a smooth decrease in photon energies between 0.1 MeV and 10 MeV (mid energy region), and at photon energies greater than 10 MeV (high energy region) has a soft increase. Maximum LAC and MAC values for the present composites were observed in the low photon energy region at 0.015 MeV. Then, it was observed that the LAC and MAC values decreased with the increase of photon energy. Above 5 MeV thereafter, the LAC and MAC values have a very weak dependence on the photon energy. This relationship of LAC and MAC to photon energy is associated with partial photon interaction. In the low photon energy region (0.015–0.4 MeV), the photoelectric effect, which is inverse to the energy (ie, $E^{-3.5}$) and depending on the atomic number as Z^{4-5}, is reported to be the main process in which photons interact with matter. In the intermediate photon energy region (0.4–5 MeV), Compton scattering is the main interaction. In this interaction, the cross section depends on the Z atomic number and the logE energy. Finally, in the high photon energy region (5–15 MeV), double generation becomes dominant, which is proportional to Z^2 and E [21].

Based on the theoretical LAC results for gamma energies between 0.015 MeV and 15 MeV, the mean free path (MFP), half value layer (HVL) and tenth value layer (TVL) were calculated for the carbide samples. The MFP values obtained for all carbide samples as a function of energy are given in Figure 2.
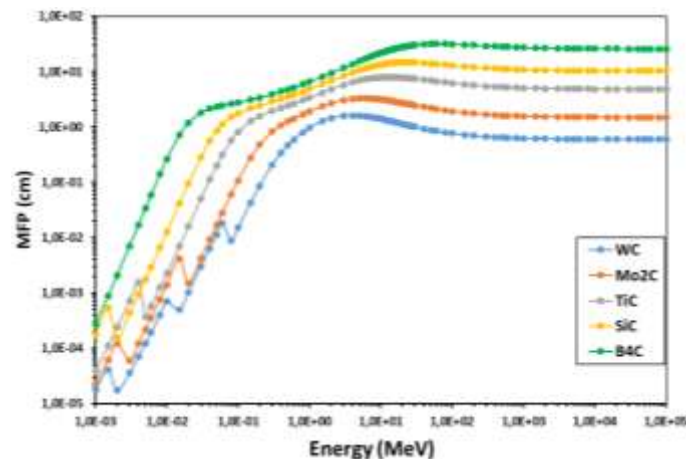

Figure 2. *MFP values as a function of photon energy for carbide samples*

From the results obtained, it is clear that the highest MFP value belongs to the B$_4$C sample and the lowest MFP value belongs to the WC sample. As can be seen from Figure 2, the distance traveled by gamma rays between two successful interactions is shorter for low-energy gamma rays and longer for high-energy gamma rays. So MFPs are proportional to increased energy. This behavior may be due to the dominance of the photoelectric effect in regions with low photon energy. Due to the dominance of Compton scattering in the mid-energy region from 0.4 to 5 MeV, a gradual increase in MFP values can be observed as the energy increases. Since pair formation predominates in the high energy region greater than 5 MeV, slight increases in MFP values may occur.

The thickness of the carbide samples used in the study was calculated to reduce the incoming gamma ray intensity by half to one tenth. The resulting HVL and TVL thicknesses are shown in Figure 3,4.
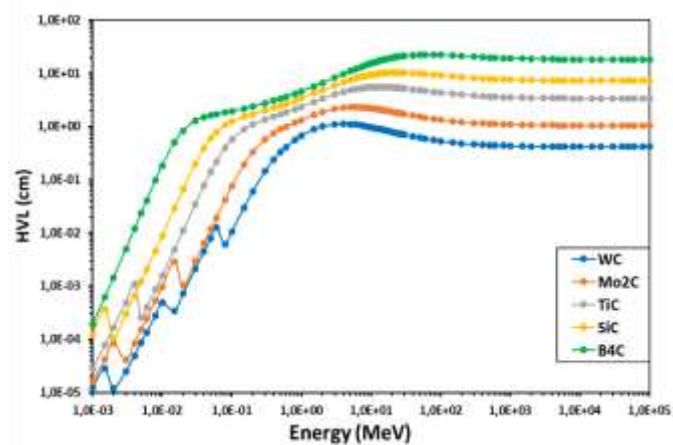
Figure 3. *HVL values as a function of photon energy for carbide samples*
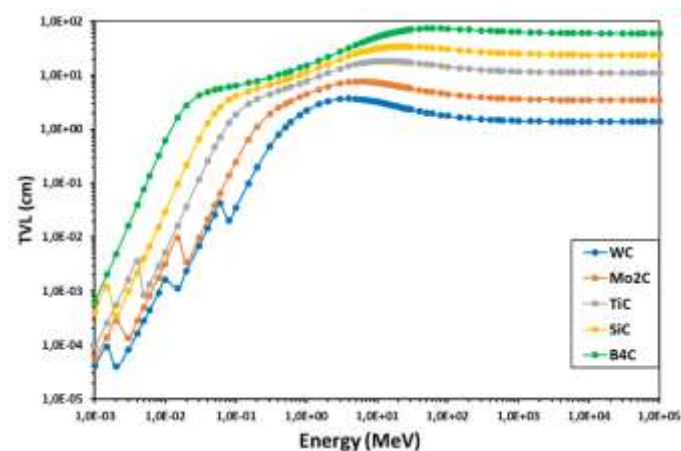

Figure 4. *TVL values as a function of photon energy for carbide samples*

As can be seen from Figure 3,4, the highest result for HVL for all gamma energies was found for the B_4C sample. It can be said that the change of HVL and TVL values depending on the energy of the gamma rays shows similar behavior with the MFP.

4. Conclusions

In this study, some radiation shielding parameters of 5 different carbide samples (such as WC, Mo_2C, TiC, SiC, B_4C) were calculated using the user-friendly online server Phy-X/PSD. The software has facilitated calculation of various important parameters such as MAC, LAC, MFP, HVL and TVL in wide energy range (i.e. 0.015 MeV–15 MeV). In light of the findings obtained from this study, it was observed that the MAC and LAC results obtained for all carbide samples decreased with increasing gamma energy. It has been revealed that MFP, HVL and TVL parameters related to the thickness of the material increase with increasing energy. In other words, it can be said that MFP, HVL and TVL values change inversely proportional to LAC values. When all parameters were evaluated, it was revealed that WC, one of the carbide samples examined in the study, had a higher performance in terms of gamma ray shielding than other samples.

Author Statements:

- **Ethical approval:** The conducted research is not related to either human or animal use.
- **Conflict of interest:** The authors declare that they have no known competing financial interests or personal relationships that could have appeared to influence the work reported in this paper
- **Acknowledgement:** The authors declare that they have nobody or no-company to acknowledge.

- **Author contributions:** The authors declare that they have equal right on this paper.
- **Funding information:** The authors declare that there is no funding to be acknowledged.
- **Data availability statement:** The data that support the findings of this study are available on request from the corresponding author. The data are not publicly available due to privacy or ethical restrictions.

References

[1]. B. Matovic, T. Yano, (2013). Silicon Carbide and Other Carbides: From Stars to the Advanced Ceramics, in: S. Somiya (Ed.), Handbook of Advanced Ceramics, second ed., Academic Press, 2013, pp. 225–244 Chap. 3.1

[2]. B. Oto, N. Yıldız, T. Korkut, E. Kavaz, (2015). Neutron shielding qualities and gamma ray buildup factors of concretes containing limonite ore, Nucl. Eng. Des. 293, 166–175.

[3]. H. Gökçe, O. Güngör, H. Yılmaz, (2021). An online software to simulate the shielding properties of materials for neutrons and photons: Ngcal, Radiat. Phys. Chem. 185, 109519.

[4]. W. Chaiphaksa, S. Yonphan, N. Chanthima, J. Kaewkhao, N. Sanwaranatee, (2022). Computational approach of alpha and proton interaction of gadolinium bismuth borate glass system using SRIM program, Mater. Today Proc. 65, 2416–2420.

[5]. M. Sayyed, K.M. Kaky, D. Gaikwad, O. Agar, U. Gawai, S. Baki, (2019). Physical, structural, optical and gamma radiation shielding properties of borate glasses containing heavy metals (Bi_2O_3/MoO_3), J. Non-Cryst. Solids 507, 30–37.

[6]. A.Mostafa, S.A. Issa, M. Sayyed, (2017). Gamma ray shielding properties of $PbO-B_2O_3-P_2O_5$ doped with WO_3, J. Alloys Compd. 708, 294–300.

[7]. O. Olarinoye, C. Oche, (2021). Gamma-ray and fast neutron shielding parameters of two new titanium-based bulk metallic glasses, Iran. J. Med. Phys. 18 (2), 139–147.

[8]. M. Al-Buriahi, Z. Alrowaili, C. Eke, J.S. Alzahrani, I. Olarinoye, C. Sriwunkum, (2022). Optical and radiation shielding studies on tellurite glass system containing ZnO and Na_2O, Optik 257, 168821.

[9]. Alım, B., (2020). A comprehensive study on radiation shielding characteristics of Tin-Silver, Manganin-R, Hastelloy-B, Hastelloy-X and Dilver-P alloys. Appl. Phys. A 126, 262. https://doi.org/10.1007/s00339-020-3442-7.

[10]. Abdel-Rahman, W., Podgorsak, E.B., (2010). Energy transfer and energy absorption in photon interactions with matter revisited: a step-by-step illustrated approach. Radiat. Phys. Chem. 79 (Issue 5), 552–566. https://doi.org/10.1016/j.radphyschem.2010.01.007.

[11]. Lakshminarayana, G., Elmahroug, Y., Kumar, Ashok, Dong, M.G., (2020). Dong-eun lee, jonghun yoon, taejoon park, $Li_2O–B_2O_3–Bi_2O_3$ glasses: gamma-rays and neutrons attenuation study using ParShield/WinXCOM program and Geant4 and penelope codes. Appl. Phys. A 126, 249. https://doi.org/10.1007/s00339-020-3418-7.

[12]. Bashter, I.I., (1997). Calculation of radiation attenuation coefficients for shielding concretes. Ann. Nucl. Energy 24, 1389.

[13]. Iskender Akkurt (2007). Effective Atomic Numbers for Fe–Mn Alloy Using Transmission Experiment Chinese Phys. Lett. 24 2812. https://doi.org/10.1088/0256-307X/24/10/027

[14]. Iskender Akkurt, (2009). "Effective atomic and electron numbers of some steels at different energies" Ann. Nucl. En. 36-11,12(2009)1702-1705 DOI: 10.1016/j.anucene.2009.09.005

[15]. Akkurt, I., Akyildirim, H., Mavi, B., Kilincarslan, S., Basyigit, C., (2010). Gamma-ray shielding properties of concrete including barite at different energies. Prog. Nucl. Energy 52 (7), 620–623.

[16]. Akkurt, I., Altindag, R., Gunoglu, K., Sarıkaya, H., (2012). Photon attenuation coefficients of concrete including marble aggregates. Ann. Nucl. Energy 43, 56–60.

[17]. Bulent Buyuk, A. Beril Tugrul, (2014). An investigation on gamma attenuation behaviour of titanium diboride reinforced boron carbide–silicon carbide composites. Radiation Physics and Chemistry 97, 354–359. http://dx.doi.org/10.1016/j.radphyschem.2013.07.025

[18]. Singh, V., Medhat, M., Shirmardi, S., (2015). Comparative studies on shielding properties of some steel alloys using Geant4, MCNP, WinXCOM and experimental results, Radiat. Phys. Chem. 106, 255-260,

[19]. İskender AKKURT, N. Ayten UYANIK, Kadir GÜNOĞLU (2015). "Radiation dose Estimation: An in vitro Measurement for Isparta-Turkey" International Journal of Computational and Experimental Science and Engineering (IJCESEN) 1-1(2015)1-4 DOI: 10.22399/ijcesen.194376

[20]. Akkurt I.;El-Khayatt A.M. Effective atomic number and electron density of marble concrete. Journal of Radioanalytical and Nuclear Chemistry. 295(1)633 – 638.. DOI: 10.1007/s10967-012-2111-5

[21]. Mahmoud, M.E., El-Khatib, A.M., Badawi, M.S., Rashad, A.R., El-Sharkawy, R.M., Thabet, A.A., (2018). Fabrication, characterization and gamma rays shielding properties of nano and micro lead oxide-dispersed-high density polyethylene composites. Radiat. Phys. Chem. 145, 160–173.

[22]. Tishkevich, D.I., Grabchikov, S.S., Lastovskii, S.B., Trukhanov, S.V., Vasin, D.S., Zubar, T.I., Kozlovskiy, A.L., Zdorovets, M.V., Sivakov, V.A., Muradyan, T.R., Trukhanov, A.V.,(2019). Function composites materials for shielding applications: correlation between phase separation and attenuation properties, J. Alloys Compd. 771, 238-245.

[23]. Albıdhanı, H., Gunoglu, K., Akkurt,İ., (2019). Natural Radiation Measurement in Some Soil Samples from Basra oil field, IRAQ State . International Journal of Computational and Experimental Science and Engineering , 5 (1) , 48-51 . DOI: 10.22399/ijcesen.498695

[24]. Tekin, H.O., Kassab, L.R.P., Kilicoglu, O., Magalhaes, E.S., Issa, S.A.M., da Silva Mattos, G.R., (2019). Newly developed tellurium oxide glasses for nuclear shielding applications: an extended investigation, J. Non-Cryst. Solids 528, 119763 1-16.

[25]. Akman, F., Kaçal, M.R., Sayyed, M.I., Karatas, H.A., (2019). Study of gamma radiation attenuation properties of some selected ternary alloys, J. Alloy. Compd. 782, 315–322.

[26]. Wen, Shao-yong, Qiao, Hong-xia, Wang, Peng-hui, Yang, Tian-xia, Yang, Zhen-qing, (2019). Electrochemical characteristic analysis of corrosion of coated steel bars in magnesium oxychloride concrete. Emerg. Mater. Res. 8–4, 696–703.

[27]. H. Alavian, H. Tavakoli-Anbaran, (2019). "Study on Gamma Shielding Polymer Composites Reinforced with Different Sizes and Proportions of Tungsten Particles Using MCNP code," Progress in Nuclear Energy, vol. 115, pp. 91-98.

[28]. Alyaa H. Abdalsalam, Erdem Şakar, Kawa M. Kakya, M.H.A. Mharebd, Betul Ceviz Şakar, M.I. Sayyed, Ali Gürol, (2020). Investigation of gamma ray attenuation features of bismuth oxide nano powder reinforced high-density polyethylene matrix composites. Radiation Physics and Chemistry 168, 108537. https://doi.org/10.1016/j.radphyschem.2019.108537

[29]. Eskalen, H., Kavun, Y., Kerli, S., Eken, S., (2020). An investigation of radiation shielding properties of boron doped ZnO thin films. Opt. Mater. 105, 109871, 1-6

[30]. Adliene, D., Gilys, L., Griskonis, E., (2020). Development and characterization of new tungsten and tantalum containing composites for radiation shielding in medicine, Nucl. Instrum. Methods Phys. Res. Sect. B Beam Interact. Mater. Atoms 467, 21–26,

[31]. Alatawi, A., Alsharari, A.M., Issa, S.A.M., Rashad, M., Darwish, A.A.A., Saddeek, Y.B., Tekin, H.O., (2020). Improvement of mechanical properties and radiation shielding performance of AlBiBO3 glasses using yttria: an experimental investigation, Ceram. Int. 46, 3534–3542,

[32]. F. Akman, M. R. Kaçal, N. Almousa, M. I. Sayyed, H. Polat, (2020). "Gamma-ray Attenuation Parameters for Polymer Composites Reinforced with BaTiO3 and CaWO4 Compounds," Progress in Nuclear Energy, vol. 121, p. 103257.

[33]. E.E. Altunsoy, H.O. Tekin, A. Mesbahi, I. Akkurt, (2020). MCNPX Simulation for Radiation Dose Absorption of Anatomical Regions and Some Organs. Acta Physica Polonica A 137-4(2020)561-565. DOI: 10.12693/APhysPolA.137.561

[34]. S. Atef, D. E. El-Nashar, A. H. Ashour, S. El-Fiki, S. U. El-Kameesy, M. Medhat, (2020). "Effect of Gamma Irradiation and Lead Content on the Physical and Shielding Properties of PVC/NBR Polymer Blends," Polymer Bulletin, vol. 77, pp. 5423–5438.

[35]. B. Ahmed, G. B. Shah, A. H. Malik, Aurangzeb, M. Rizwan, (2020). "Gamma-ray Shielding Characteristics of Flexible Silicone Tungsten Composites," Applied Radiation and Isotopes, vol. 155, p. 108901.

[36]. Rammah, Y.S., El-Agwany, F.I., Mahmoud, K.A., Novatski, A., El-Mallawany, R., (2020). Role of ZnO on TeO2.Li2O.ZnO glasses for optical and nuclear radiation shielding applications utilizing MCNP5 simulations and WINXCOM program, J. Non-Cryst. Solids 544, 120162,

[37]. Malidarre, R.B., Akkurt, I., Kavas, T., (2021) Monte Carlo simulation onshielding properties of neutron-gamma from 252Cf source for Alumino-Boro-Silicate Glasses, Radiation Physics and Chemistry,186, 109540. https://doi.org/10.1016/j.radphyschem.2021.109540

[38]. Gunoglu K., Varol Ozkavak H., Akkurt I., (2021). Evaluation of gamma ray attenuation properties of boron carbide (B4C) doped AISI 316 stainless steel: Experimental, XCOM and Phy-X/PSD database software. Materials Today Communications 29, 102793, 1-9.

[39]. Akkurt, I., Malidarre, R.B. & Kavas, T., (2021). Monte Carlo simulation of radiation shielding properties of the glass system containing Bi2O3. Eur. Phys. J. Plus 136, 264. https://doi.org/10.1140/epjp/s13360-021-01260-y

[40]. Şen Baykal, D., Tekin, H.O., Çakırlı Mutlu, R., (2021). An Investigation on Radiation Shielding Properties of Borosilicate Glass Systems . International Journal of Computational and Experimental Science and Engineering, 7 (2) , 99-108 . DOI: 10.22399/ijcesen.960151

[41]. Akkurt, R.B. Malidarre, I. Kartal, K. Gunoglu, (2021).Monte Carlo simulations study on gamma ray–neutron shielding characteristics for vinyl ester composites Polymer Composites . 2021;42:4764–4774. https://doi.org/10.1002/pc.26185

[42]. Zarkooshi, A. , Latıf, K. H. & Hawı, F. (2021). Estimating the Concentrations of Natural Isotopes of 238 U and 232Th and Radiation Dose Rates for Wasit Province-Iraq by Gr-460 system . International Journal of Computational and Experimental Science and Engineering , 7 (3) , 128-132 . DOI: 10.22399/ijcesen.891935

[43]. Akkurt, I., Gunoglu, K., (2021). Radiation shielding properties of concrete containing magnetite. Progress in Nuclear Energy 137, 103776, 1-8.

[44]. Kurtulus, R., Kavas, T., Akkurt, I. et al., (2021). A comprehensive study on novel alumino-borosilicate glass reinforced with Bi2O3 for radiation shielding applications: synthesis, spectrometer, XCOM, and MCNP-X works. J Mater Sci: Mater Electron 32, 13882–13896. https://doi.org/10.1007/s10854-021-05964-w

[45]. Boodaghi Malidarre, R. , Akkurt, İ. , Gunoglu, K. & Akyıldırım, H. (2021). Fast Neutrons Shielding Properties for HAP-Fe2O3 Composite Materials . International Journal of Computational and Experimental Science and Engineering , 7 (3) , 143-145 . DOI: 10.22399/ijcesen.1012039

[46]. Ezgi Eren Belgin, (2022). Comparison of gamma spectrometric method and XCOM method in calculating mass attenuation coefficients of reinforced polymeric composite materials. Radiation Physics and Chemistry 193, 109960. https://doi.org/10.1016/j.radphyschem.2022.109960

[47]. Vignesh S., Winowlin Jappes JT., Nagaveena S., Krishna Sharma R., Adam Khan M. (2022). Boron carbide dispersed epoxy composites for gamma radiation shielding applications. Vacuum 205, 111474, 1-5. https://doi.org/10.1016/j.vacuum.2022.111474

[48]. Zübeyde Özkan, Uğur Gökmen, Sema Bilge Ocak, (2023). Analyses of Gamma and Neutron Attenuation Properties of the AA6082 composite material doped with boron carbide (B4C). Radiation Physics and Chemistry 206, 110810. https://doi.org/10.1016/j.radphyschem.2023.110810

[49]. I.A. El-Mesady, Y.S. Rammah, A.E. Hussein, H.M. El-Samman, F.I. El-Agawany, R.A. Elsad, (2023). Synthesis, optical, mechanical characteristics, and gamma-ray shielding capacity of polyethylene -basalt mixture. Radiation Physics and Chemistry 209, 110974, https://doi.org/10.1016/j.radphyschem.2023.110974

[50]. N. Sabry, I.S. Yahia, (2023). Attenuation features of Ag2ZnSnS4, Ag2ZnSnSe4, ZnS, and Ag2S compounds against indirect ionizing radiation using Phy-X/PSD software. Physica B 650, 414526. https://doi.org/10.1016/j.physb.2022.414526

[51]. Oruncak, B. (2023). Computation of Neutron Coefficients for B2O3 reinforced Composite . International Journal of Computational and Experimental Science and Engineering , 9 (2) , 50-53 . DOI: 10.22399/ijcesen.1290497

[52]. Aygun, Z. & Aygün, M. (2023). An Analysis on Radiation Protection Abilities of Different Colored Obsidians . International Journal of Computational and Experimental Science and Engineering , 9 (2) , 170-176 . DOI: 10.22399/ijcesen.1076556

[53]. Muhammed Fatih Kuluöztürk (2023). Optimization of 3×3 inch NaI(Tl) detector related to energy, distance and bias voltage. Journal of Radiation Research and Applied Sciences 16(3);100613. https://doi.org/10.1016/j.jrras.2023.100613

[54]. Yonca Yahsi Celen, Sule Oncul, Barıs Narin, Osman Gunay. (2023). Measuring radon concentration and investigation of it's effects on lung cancer. Journal of Radiation Research and Applied Sciences16(4);100716. https://doi.org/10.1016/j.jrras.2023.100716

[55]. Aycan Şengül. (2023). Gamma-ray attenuation properties of polymer biomaterials: Experiment, XCOM and GAMOS results. Journal of Radiation Research and Applied Sciences 16(4);100702. https://doi.org/10.1016/j.jrras.2023.100702

[56]. Nurdan Karpuz. (2023). Radiation shielding properties of glass composition. Journal of Radiation Research and Applied Sciences 16(4);100689 https://doi.org/10.1016/j.jrras.2023.100689

[57]. G. ALMisned, K. Günoğlu, H. Varol Özkavak, D. Sen Baykal, H.O. Tekin, N. Karpuz, I. Akkurt, (2023).An investigation on gamma-ray and neutron attenuation properties of multi-layered Al/B4C composite, Materials Today Communications, 36, 106813

[58]. Şengül, I. Akkurt, K. Gunoglu, K. Akgüngör, R.B. Ermis, (2023). Experimental evaluation of gamma-rays shielding properties of ceramic materials used in dentistry, Radiation Physics and Chemistry, 204, 110701

[59]. S¸Akar, E., Özpolat, Ö.F., Alım, B., Sayyed, M.I., Kurudirek, M., (2020). Phy-X/PSD: development of a user friendly online software for calculation of parameters relevant to radiation shielding and dosimetry. Radiat. Phys. Chem. 166, 108496. https://doi.org/10.1016/j.radphyschem.2019.108496.